DOI: https://doi.org/10.24425/amm.2025.156240

C.C. CHANG^{0,1}, M.F. MOHD NAZERI^{0,2}, M.A.F.M. MUKHTAR^{0,1}, A. ALSHOAIBI^{0,3}, Y. TABAK^{0,4}, A. EVCIN^{0,5}, F. HUSSAIN^{0,6}, A.A. MOHAMAD^{0,1,7*}

INTERMETALLIC COMPOUND GROWTH, HARDNESS AND CORROSION PROPERTIES OF SAC305/CU SOLDER BY MICROWAVE HYBRID HEATING

Tin-silver-copper (Sn-3.0Ag-0.5Cu, SAC305) in the form of SAC305/Cu joint were compared under different reflowing conditions; conventional reflow (CR) and microwave hybrid heating (MR). The results showed that both reflow methods produced an interfacial and primary intermetallic compound (IMC) layer, specifically η -Cu₆Sn₅, which contributed to increased sample hardness. However, extended MR reflow times led to the formation of ε -Cu₃Sn, which could potentially reduce solder joint reliability. Notably, after exposure to corrosion, the samples exhibited minimal pitting, indicating enhanced corrosion resistance following MR reflow. This improvement is likely due to the more prominent IMC presence in MR compared to CR.

Keywords: Intermetallic compound; Hardness; Corrosion; Microwave hybrid heating

1. Introduction

Microwave hybrid heating (MR) is recognized as a favorable alternative to conventional reflow (CR) methods due to its advantages, such as uniform heating, energy efficiency, and shorter processing time [1]. It has been suggested that the shorter processing time is particularly beneficial for sensitive electronic components [2,3]. However, it is crucial to carefully manage the processing time to prevent brittleness caused by crack initiation and excessive intermetallic compound (IMC) formation between Sn-3.0Ag-0.5Cu (SAC305) solder and the copper (Cu) plate. Despite the numerous advantages MR offers, there is limited information regarding the optimization of the reflow process for SAC305 solder on a deposited Cu substrate.

The choice of reflow method, whether MR or CR, can significantly impact the properties of solder joints, affecting their performance and reliability [4,5]. The distinct heating mechanism of MR compared to CR can lead to differences in microstructure, hardness, and corrosion resistance. Investigating these variations

is crucial, as hardness influences wear resistance and durability, while corrosion resistance determines the long-term reliability of solder joints, particularly in harsh environments [6,7]. Understanding these effects will aid in optimizing reflow processes for improved solder joint performance.

Researchers have highlighted MR showing the potential for reduced IMC thickness and improved uniformity, and enhances microstructural refinement in the solder matrix, which contributes to increased joint hardness and better fatigue resistance [8]. Additionally, shorter processing times of MR and lower thermal gradients have been linked to reduced void formation and improved wettability in solder joints [9]. In terms of corrosion resistance, recent studies suggest that the refined microstructure and controlled IMC growth contribute to better resistance against chloride-induced corrosion, making it a promising method for ensuring solder joint reliability in aggressive environments [10]. Therefore, this study investigates the effects of MR on the IMC, hardness, and corrosion of SAC305/Cu joints, comparing these results with those from the CR process.

^{*} Corresponding author: aam@usm.my



¹ UNIVERSITI SAINS MALAYSIA, ENERGY MATERIALS RESEARCH GROUP (EMRG), SCHOOL OF MATERIALS AND MINERAL RESOURCES ENGINEERING, PULAU PINANG, MALAYSIA

UNIVERSITI MALAYSIA PERLIS (UNIMAP), FACULTY OF CHEMICAL ENGINEERING AND TECHNOLOGY, SURFACE TECHNOLOGY SPECIAL INTEREST GROUP, 02600, ARAU, PERLIS MALAYSIA

FERLIS, MALATSIA

SING FARISAL UNIVERSITY, DEPARTMENT OF PHYSICS, COLLEGE OF SCIENCE, AL-HASSA, P.O. BOX 400, HOFUF, 31982, SAUDI ARABIA

TUBITAK NATIONAL METROLOGY INSTITUTE (TUBITAK UME), KOCAELI 41470, TÜRKIYE

AFYON KOCATEPE UNIVERSITY, DEPARTMENT OF MATERIALS SCIENCE AND ENGINEERING, AFYON 03200, TURKIYE

⁶ NED UNIVERSITY OF ENGINEERING AND TECHNOLOGY, DEPARTMENT OF MATERIALS ENGINEERING, KARACHI, 75270, PAKISTAN

CHULALONGKORN UNIVERSITY, FACULTY OF ENGINEERING, DEPARTMENT OF CHEMICAL ENGINEERING, BANGKOK 10330, THAILAND

2. Experimental

A 3 cm × 2 cm Cu plate was cleaned with ethanol using ultrasonic machine, and SAC305 solder paste (Alpha CVP 390) was applied with a stencil thickness 1 mm to achieve a uniform surface (Fig. 1). For conventional reflow (CR), the SAC305/Cu samples were heated at 250°C for 6 minutes (360 seconds) in a Reflow Oven T200N+. Meanwhile, for microwave hybrid reflow (MR), the process was conducted using high heating mode at 50, 100, 150, 200, and 250 seconds with a Panasonic NN-ST34HM (2.45 GHz, 800 W).

All reflowed samples were examined using a field emission scanning electron microscope (FESEM, Zeiss SupraTM 35VP), with micrographs captured in backscattered mode. X-ray diffraction (XRD) analysis (Bruker AXS D9 Diffractometer) was performed for phase identification, with a scanning angle of 2θ ranging from 10° to 90° .

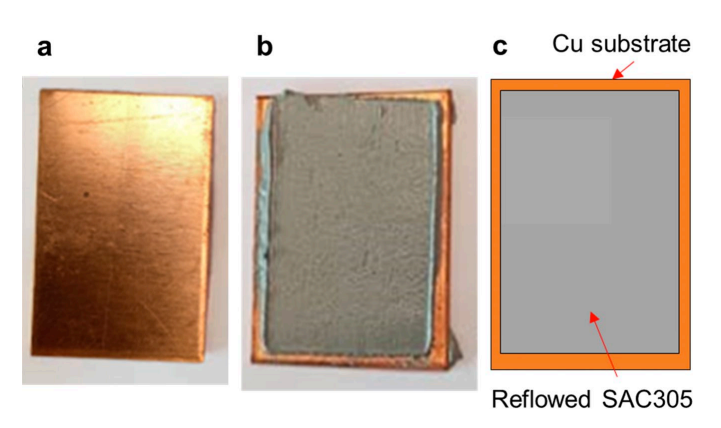


Fig. 1. (a) Cu substrate, (b) solder paste printed on the Cu substrate, and (c) schematic diagram of the reflowed sample on the Cu substrate

For Vickers hardness measurement, the surface of the reflowed samples was tested using a Vickers hardness machine (LV Series, Leco) with a force of 0.03 kgf applied. For the nanoindenter test (Micro Materials), the mounted reflowed samples were used for measurement, with a force of 20 N applied to the marked area and a dwell time of 10 seconds. The galvanic corrosion test was performed in a 3.5 wt.% NaCl solution, using a multimeter to measure the corrosion current between the Cu plate and all the studied samples. The metastable pitting rate (MPR) was obtained by dividing the number of transient peaks recorded by the test duration.

3. Results and discussions

3.1. Microwave Reflow

To evaluate the application of MR, the sample processed by CR was used for comparison (Fig. 2). At 50s, both CR and MR samples showed yellowish residues, indicating incomplete flux reaction during reflow (Fig. 2a). With increased reflow time, the flux received enough heat to burn completely, changing from

a yellowish to a blackish substance (Fig. 2b-c). However, this residue did not uniformly cover the entire surface of the MR samples, as observed with different reflow times. Some of the burnt flux became trapped beneath a thin Sn surface, forming an 'island' structure (Fig. 2c-f). During microwave reflow, the flux combusted and was released into the air, leaving a black burnt mark on the surface of the sample, which caused inward shrinkage of the solder paste. The uneven distribution of SAC305 solder particles across the sample led to inconsistent flux evaporation, resulting in uneven shrinkage and a rougher surface texture.

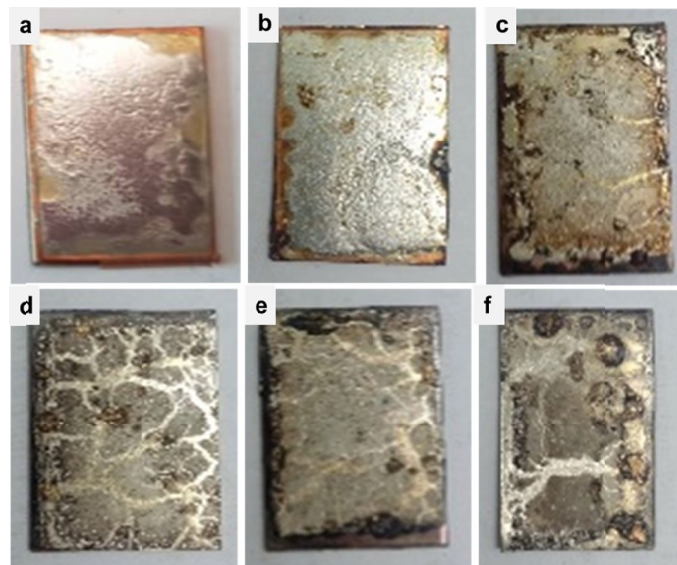


Fig. 2. Conventional reflow (a) CR-360s and MR samples with reflow time of (b) 50s, (c) 100s, (d) 150s, (e) 200s and (f) 250s

3.2. Top View Morphology

The CR-SAC305/Cu sample (Fig. 3a) is characterized by a sparse distribution of $\eta\text{-}Cu_6Sn_5$ within the $\beta\text{-}Sn$ matrix compared with MR. Since CR uses a slower heat transfer rate via convection to melt the solder paste, heat energy is released into the surroundings [11]. The released heat energy is partially lost to the surroundings due to the slow transfer rate and prolonged heating time. Slower heating may cause partial melting, leading to a non-homogeneous distribution of phases, potentially affecting microstructure formation. Similar findings have been reported by other researchers, where slower heating in CR results in uneven growth of IMC, leading to a microstructure with lower homogeneity and mechanical reliability [12].

The ratio of η -Cu₆Sn₅ phase to β -Sn phase increases with longer reflow times under microwave reflow (Fig. 3b-f). Additionally, the presence of white and elongated form associated with "needle-like" structure of the Ag₃Sn phase was detected multiply at 50 seconds of. The η -Cu₆Sn₅ phases become more irregular. Microwave energy heats the solder paste faster than conventional methods [13]. This difference in heating produces distinct surface morphologies between the two reflow meth-

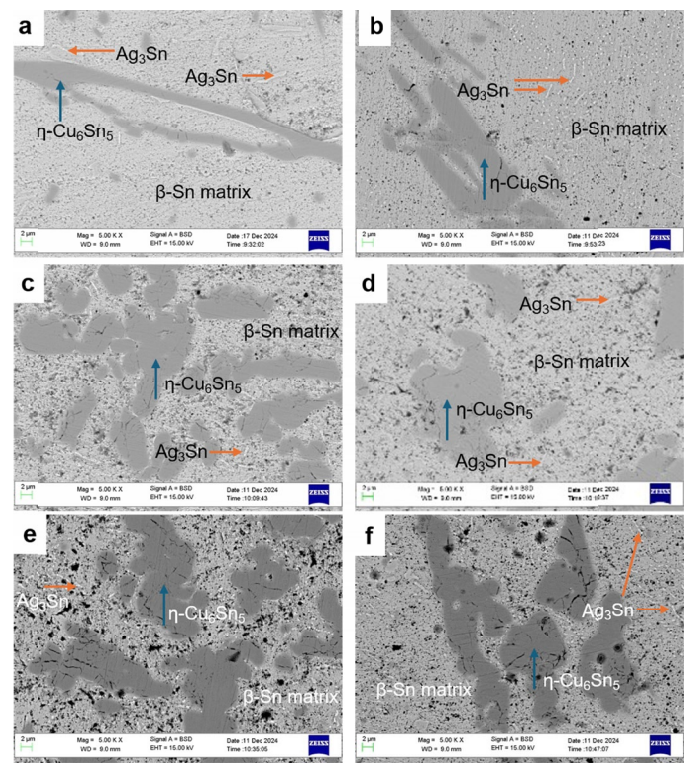


Fig. 3. Surface FESEM micrographs of (a) CR-SAC305/Cu sample, (b) 50s MR-SAC305/Cu sample, (c) 100s MR-SAC305/Cu sample, (d) 150s MR-SAC305/Cu sample, (e) 200s MR-SAC305/Cu sample and (f) 250s MR-SAC305/Cu sample

ods. Similar trends have been observed, where rapid heating in advanced reflow techniques such as microwave or infrared heating leads to more refined and uniform distributions of IMC compared to CR [14].

The η -Cu₆Sn₅ phase grows with longer reflow times, transitioning from isolated grains to a rough, scallop-like structure. This explains the more dominant presence of η -Cu₆Sn₅ on the surface of MR-SAC305/Cu samples. Researchers have consistently linked scallop-like IMC morphologies to enhanced diffusion at higher reflow temperatures, which occur more effectively under microwave reflow due to its efficient and localized heating [15].

3.3. Cross Section Morphology

To study IMC formation, the samples were cross-sectioned (Fig. 4a-c) and observed by FESEM (Fig. 4d-i). The cross-sectional analysis of the reflowed CR and MR samples revealed three distinct layers: the SAC solder layer, the interfacial IMC layer, and the Cu layer (Fig. 4c). As reflow time increased, Cu atoms diffused into the solder, promoting the formation of the interfacial IMC layer between the Cu substrate and the solder surface. A single interfacial IMC layer consisting of the $\eta\text{-Cu}_6\text{Sn}_5$ was observed in between SAC solder layer and Cu layer in samples CR and MR with reflow times of 100 s or less (Fig. 4d-f). A comparative analysis at 50 s showed that MR samples exhibited a more continuous and uniform $\eta\text{-Cu}_6\text{Sn}_5$

layer (3.06 µm thickness average) compared to the CR samples (2.35 µm thickness average), where the IMC layer appeared thinner and less homogeneous. This difference is attributed to the faster and more localized heating provided by MR, which accelerates the diffusion of Cu into the molten solder and promotes uniform IMC formation [16].

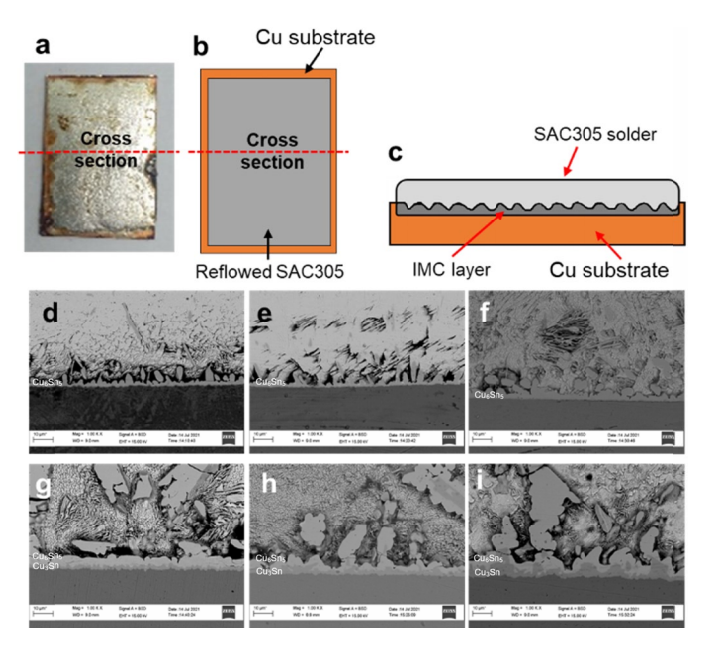


Fig. 4. (a) reflowed CR sample, (b) schematic diagram of reflowed sample on Cu substrate; (c) schematic diagram of cross-sectioned samples; FESEM cross-section micrograph of CR reflow (d) and MR reflow at (e) 50s, (e) 50s, (f) 100s, (g) 150s, (h) 200s and (i) 250s

While at MR with reflow times of 150 s or more, two interfacial IMC layers appeared in the samples where one consist of η -Cu₆Sn₅ and another one consists of ϵ -Cu₃Sn (Fig. 4g-i). The bright IMC layer was identified as the η -Cu₆Sn₅ phase, and the darker layer as the ϵ -Cu₃Sn phase. These observations align with findings from other researchers, where extended reflow times under rapid heating conditions favor the formation of a secondary ϵ -Cu₃Sn layer due to enhanced diffusion kinetics and prolonged reaction times [17].

In addition to the interfacial IMC layer, primary IMC grains were also observed within the Sn layer in all reflowed samples. These grains formed due to the reaction between Sn and Cu atoms diffused from the Cu substrate, resulting in irregular $\eta\text{-Cu}_6\text{Sn}_5$ grains. As reflow time increased under MR, the number of IMC grains decreased, but their size grew, with the $\epsilon\text{-Cu}_3\text{Sn}$ phase appearing at the center of these grains after 100 s. Kirkendall voids due to Cu and Sn diffusion rate differences were seen in the MR-SAC305/Cu IMC layer, which may cause brittle fractures and connectivity loss [18].

3.4. Hardness analysis

For the Vickers hardness measurement, five random points on the surface of the reflowed samples were measured using Bulk

solder

a

Measurement

points

a Vickers hardness machine (Fig. 5a). For the nano-indenter test, mounted reflowed samples were used for cross-sectional measurement (Fig. 5b). The average Vickers hardness of CR on the top (7.344 HV) and MR 50 s on the cross-section (10.964 HV) reveals that MR produces samples that are almost 40% harder than the CR-SAC305/Cu samples (Fig. 5c). Note that the hardness steadily increases with MR time, reaching a maximum hardness of 13 HV for the sample reflowed for 250 s (Fig. 5d). The top layer of the CR-SAC305/Cu sample exhibited the lowest nano-indentation hardness of 0.2 GPa (Fig. 5e), consistent with a previous report [19].

For the MR-SAC305/Cu samples, the hardness marginally increased from 0.24 GPa to 0.35 GPa as the reflow time increased, a trend similar to that observed in the Vickers hardness measurements. The hardness in the middle and bottom regions also shows an increasing trend. Moreover, these areas contained a high concentration of primary and interfacial η -Cu₆Sn₅ IMCs. The presence of both primary and interfacial η -Cu₆Sn₅ IMCs acts

b

15 measurement points

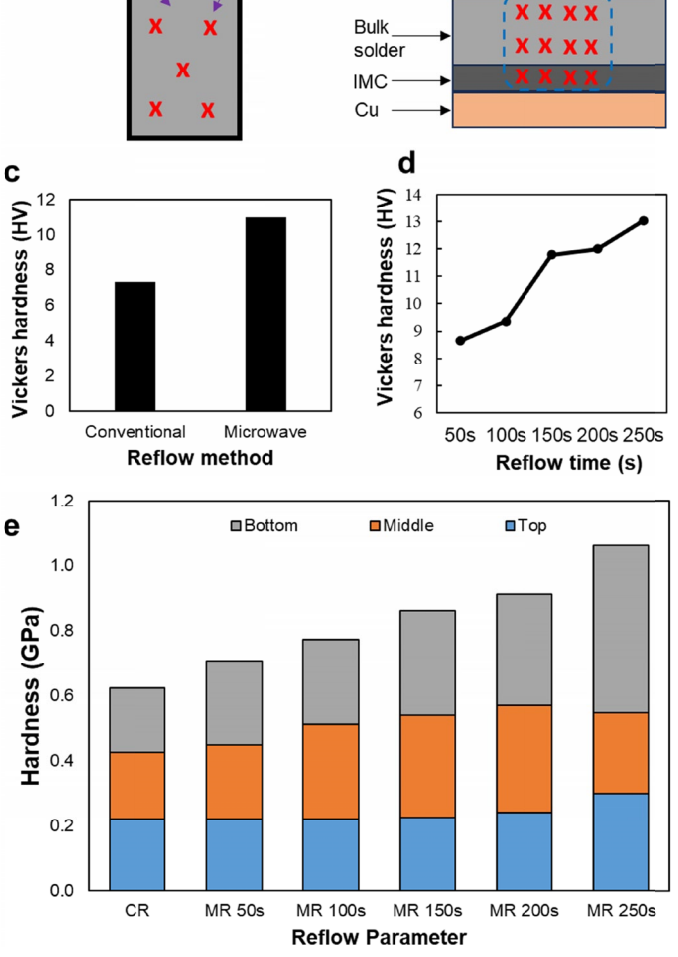


Fig. 5. Schematic diagrams of (a) top section Vickers hardness measurement points, (b) cross-section of hardness measurement points, (c) Comparison of average Vickers hardness of CR-SAC305/Cu sample and MR-SAC305/Cu samples (top surface), (d) Vickers hardness of MR-SAC305/Cu samples with different reflow time and (e) nanoindentation hardness at different layers

as a barrier to dislocation movement in the β -Sn grains. As the number of η -Cu₆Sn₅ grains increases with longer reflow times, dislocation slip becomes more difficult, resulting in an increase in the hardness of the samples [20].

3.5. Corrosion analysis

The corrosion current for all samples fluctuates during the first 30 minutes of immersion in a 3.5% NaCl solution, then gradually stabilizes (Fig. 6). This initial period is critical for investigating the formation of metastable pitting [21,22]. The CR-SAC305/Cu sample produces three current transient peaks within the first 30 minutes (insert Fig. 6a1), while only two peaks are observed for the MR-SAC305/Cu 50s sample (Fig. 6b). As the reflow time increases, the number of peaks remains between 2 and 3 for all samples. Further EDX analysis of the corrosion products suggests that higher amounts of chlorine were present in the CR-SAC305/Cu sample (Fig. 6c), indicating that the MR samples have slightly better resistance to pitting corrosion. The increasingly dominant IMC of η-Cu₆Sn₅ may contribute to the improved corrosion resistance of the MR samples. Interestingly, all samples were found to produce the same corrosion products: Sn₃O(OH)₂Cl₂ (ICDD 98-000-6006) (Fig. 6d).

When the reflowed SAC305/Cu sample was immersed in the NaCl solution, Sn^{2+} ions dissolved into the solution and reacted with both Cl^- and OH^- ions to form the corrosion products. The Cl^- ions began attacking the passivation oxide layer, particularly at the intergranular boundaries or surface discontinuities of the corrosion product, which served as effective diffusion paths for Cl^- ions. This facilitated the pitting process and led to the formation of deeper pits along the intergranular boundaries inside the underlying SAC305 solder layer [23]. A competing process between pitting and re-passivation of the corrosion product occurred, producing the oxy-hydrochloride phase of $Sn_3O(OH)_2Cl_2$ via reaction (1) [24]:

$$3\text{Sn} + 4\text{OH}^- + 2\text{Cl}^- \rightarrow \text{Sn}_3\text{O(OH)}_2\text{Cl}_2 + \text{H}_2\text{O} + 6\text{e}^-$$
 (1)

4. Conclusion

In this study, different reflowing methods were utilized to investigate changes in IMC growth in SAC305/Cu joints. The findings are summarized as follows;

- The η-Cu₆Sn₅ IMC grew significantly in the bulk solder with longer MR reflow times, increasing solder joint hardness.-
- ii. MR samples exhibited higher chlorine content in the corrosion products, indicating slightly lower pitting resistance, although they produced the same phase of corrosion product as the CR samples.

These results suggest that the MR method shows significant promise for reflowing solder alloys. However, careful management of reflow time is essential to prevent excessive IMC growth.

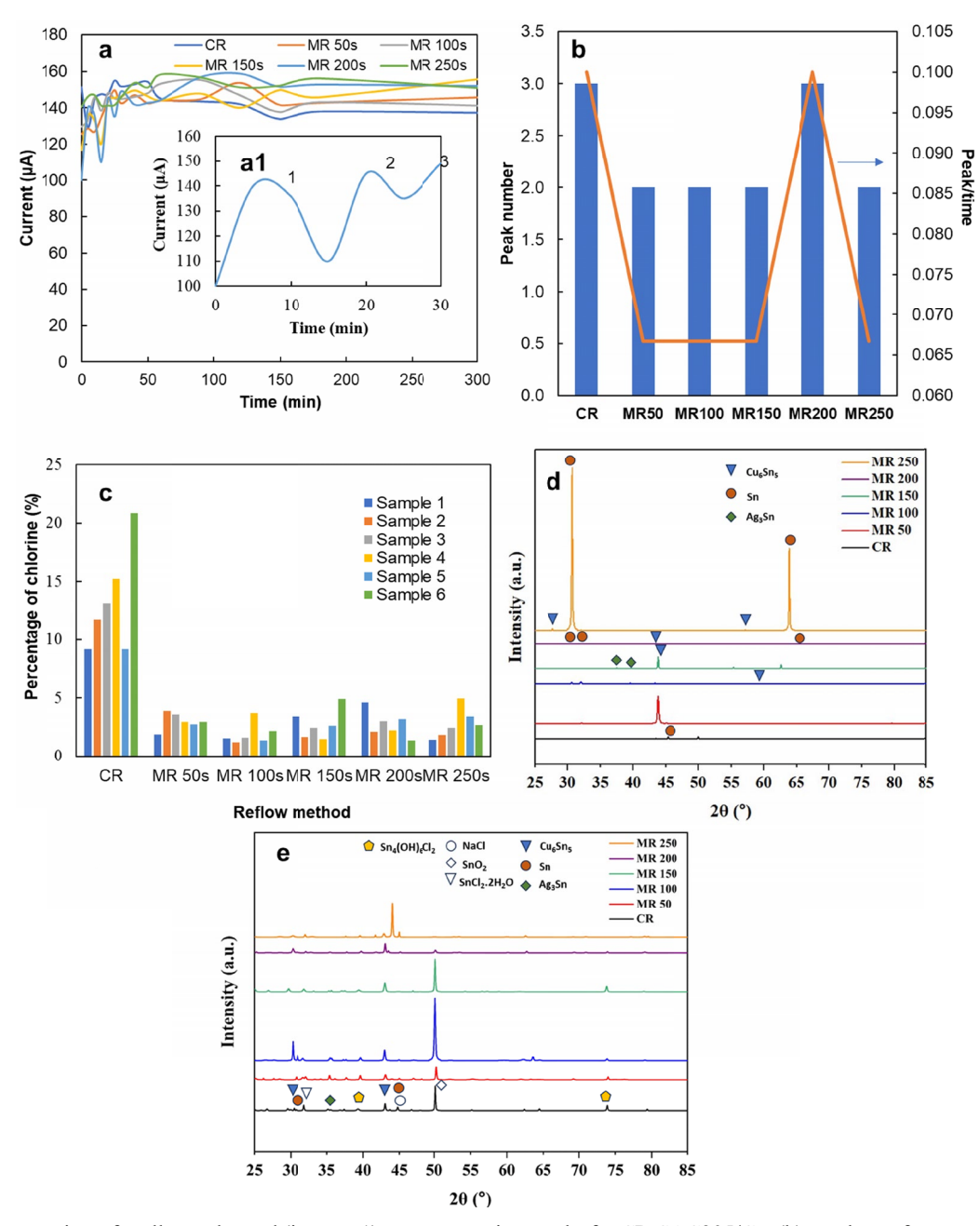


Fig. 6. (a) Current transients for all samples and (insert, a1) current transient peaks for CR-SAC305/Cu, (b) numbers of current transient peaks in the first 30 mins, (c) post-corrosion chlorine elemental analysis, (d) pre-corrosion phase determination and (e) post-corrosion test phase

Acknowledgement

Special thanks to Universiti Sains Malaysia for Internationalisation Incentive Scheme provided (R502-KR-ARP004-00AUPRM003-K134). This work was supported by the Deanship of Scientific Research, Vice Presidency for Graduate Studies and Scientific Research, King Faisal University, Saudi Arabia [Grant No. KFU241934].

REFERENCES

[1] M. Said, N.M. Sharif, M.F.M. Nazeri, S. Kheawhom, A.A. Mohamad, Comparison of Intermetallic Compound Growth and Tensile Behavior of Sn-3.0 Ag-0.5 Cu/Cu Solder Joints by Conventional and Microwave Hybrid Heating. J. Mater. Res. Technol. **17**, 1438-1449 (2022).

DOI: https://doi.org/10.1016/j.jmrt.2022.01.085

- [2] L. Mei Lee, H. Haliman, A.A. Mohamad, Interfacial Reaction of a Sn-3.0 Ag-0.5 Cu Thin Film During Solder Reflow. Solder Surf. Mt. Tech. 25 (1), 15-23 (2013).
 - DOI: https://doi.org/10.1108/09540911311294560
- [3] L.M. Lee, A.A. Mohamad, Interfacial Reaction of Sn-Ag-Cu Lead-Free Solder Alloy on Cu: A Review. Adv. Mater. Sci. Eng 25, 123697 (2013). DOI: https://doi.org/10.1155/2013/123697
- [4] M. Said, N.A. Salleh, M.F.M. Nazeri, H. Akbulut, S. Kheawhom, A.A. Mohamad, Microwave Hybrid Heating for Lead-Free Solder: A Review. J. Mater. Res. Technol. 26, 6220-6243 (2023). DOI: https://doi.org/10.1016/j.jmrt.2023.08.299

- [5] S.S.M. Nasir, M.Z. Yahaya, A.M. Erer, B. Illés, A.A. Mohamad, Effect of TiO₂ Nanoparticles on The Horizontal Hardness Properties Of Sn-3.0 Ag-0.5 Cu-1.0 TiO₂ Composite Solder. Ceram. Int. 45 (15), 18563-18571 (2019). DOI: https://doi.org/10.1016/j.ceramint.2019.06.079
- [6] M. Said, M.F.M. Nazeri, N.M. Sharif, S. Kheawhom, A.A. Mohamad, Corrosion Properties Of Cu/Sn-3.0 Ag-0.5 Cu/Cu Solder Butt Joints Fabricated By Conventional Reflow And Microwave
 - Hybrid Heating. Corros. Sci. **208**, 110641 (2022). DOI: https://doi.org/10.1016/j.corsci.2022.110641
- [7] M.F. Mohd Nazeri, M.Z. Yahaya, A. Gursel, F. Cheani, M.N. Masri, A.A. Mohamad, Corrosion Characterization of Sn-Zn Solder: A Review, Solder Surf. Mt. Tech. 31 (1), 52-67 (2019). DOI: https://doi.org/10.1108/ssmt-05-2018-0013
- [8] M. Yuan, S. Cai, C. Li, X. Wang, C. Liu, Y. Qiao, X. Pang, E.R. Elsharkawy, B. Liu, J. Zhang, Influence of Trace Mn Doping on The High-Speed Shear Performance of Lead-Free Alloy/Copper Solder Joints: Experimental And First Principles Investigation. Surfaces and Interfaces 51, 104477 (2024). DOI: https://doi.org/10.1016/j.surfin.2024.104477
- [9] N. Ismail, W.Y.W. Yusoff, N.A.A. Manaf, A. Amat, N. Ahmad, E.M. Salleh, A Comprehensive Review of Radiation Effects on Solder Alloys and Solder Joints. Defence Technology 39, 86-102 (2024). DOI: https://doi.org/10.1016/j.dt.2024.02.007
- [10] P. Wang, J. Zhao, L. Ma, X. Cheng, X. Li, Effect of grain ultrarefinement on microstructure, tensile property, and corrosion behavior of low alloy steel. Mater. Charact. 179, 111385 (2021). DOI: https://doi.org/10.1016/j.matchar.2021.111385
- [11] E. Calabro, S. Magazu, Comparison Between Conventional Convective Heating and Microwave Heating: An FTIR Spectroscopy Study of the Effects of Microwave Oven Cooking of Bovine Breast Meat. Journal of Electromagnetic Analysis and Applications 4 (11), 433-439 (2012).
 DOI: https://doi.org/10.4236/jemaa.2012.411060
- [12] M.I.I. Ramli, M.A.A.M. Salleh, M.M.A.B. Abdullah, N.S.M. Zaimi, A.V. Sandu, P. Vizureanu, A. Rylski, S.F.M. Amli, Formation And Growth of Intermetallic Compounds in Lead-Free Solder Joints: A Review. Materials 15 (4), 1451 (2022).
 DOI: https://doi.org/10.3390/ma15041451
- [13] J. Sun, W. Wang, Q. Yue, Review on Microwave-Matter Interaction Fundamentals and Efficient Microwave-Associated Heating Strategies. Materials 9 (4), 231 (2016).
 DOI: https://doi.org/10.3390/ma9040231
- [14] B. Chen, Y. Huang, S. Tang, W. Liu, Y. Ma, Tuning The Microstructure and Enhancing The Mechanical Properties of Au-20Sn/Au/Ni (P)/Kovar Joint by Ultrasonic-Assisted Soldering Method. J. Mater. Res. Technol. 14, 703-718 (2021).
 DOI: https://doi.org/10.1016/j.jmrt.2021.06.100

- [15] Y. Wu, Z. Zhang, L. Chen, S. Zhang, Comparative Study on The Bonding Property of Laser and Reflow Soldered Sn-3.0 Ag-0.5 Cu/Ni-P Microbumps After Isothermal Aging And Multiple Reflowing. J. Mater. Res. Technol. 29, 2868-2878 (2024). DOI: https://doi.org/10.1016/j.jmrt.2024.01.273
- [16] J. Wang, W. Chen, D. Liu, C. Li, J. Zhou, Z. Zhang, B. Chen, X. Jiang, X. Hu, Effect of the Ultrasonic-Assisted Soldering On The Interfacial Reaction and IMC Growth Behavior of SAC305 Solder With Cu Alloy Substrates. J. Mater. Sci.: Mater. Electron. 34 (20), 1517 (2023).
 DOI: https://doi.org/10.1007/s10854-023-10959-w
- [17] W. Liu, Z. Wen, J. Xu, X. Wang, R. An, C. Wang, Z. Zheng, W. Zhang, Y. Tian, Rapid Fabrication of Cu/40-μm Thick Full Cu₃Sn/Cu Joints by Applying Pulsed High Frequency Electromagnetic Field for High Power Electronics. Mater. Chem. Phys. 276, 125386 (2022).
 DOI: https://doi.org/10.1016/j.matchemphys.2021.125386
- [18] S.C. Yee, K.M.C. Wong, G. Issabayeva, A Study on the Shear Strength and Failure Modes of Sn-3.0 Ag-0.5 Cu Solder Joint Containing Pt. IOP Conf. Ser. Mater. Sci. Eng. 495, p. 012085 (2019). DOI: https://doi.org/10.1088/1757-899x/495/1/012085
- [19] S. Li, Y. Liu, H. Zhang, H. Cai, F. Sun, G. Zhang, Microstructure and Hardness of SAC305 and SAC305-0.3Ni solder on Cu, High Temperature Treated Cu, and Graphene-Coated Cu Substrates. Results Phys. 11, 617-622 (2018). DOI: https://doi.org/10.1016/j.rinp.2018.10.005
- [20] X. Wang, Y. Liu, C. Wei, H. Gao, P. Jiang, L. Yu, Strengthening Mechanism of SiC-Particulate Reinforced Sn-3.7 Ag-0.9 Zn Lead-Free Solder, J. Alloys Compd. 480 (2), 662-665 (2009). DOI: https://doi.org/10.1016/j.jallcom.2009.02.002
- [21] R.K. Gupta, B.R.W. Hinton, N. Birbilis, The Effect of Chromate on the Pitting Susceptibility of AA7075-T651 Studied Using Potentiostatic Transients. Corros. Sci. 82, 197-207 (2014). DOI: https://doi.org/10.1016/j.corsci.2014.01.012
- [22] A. Wierzbicka-Miernik, J. Guspiel, L. Zabdyr, Corrosion Behavior of Lead-Free SAC-Type Solder Alloys in Liquid Media. Arch. Civ. Mech. Eng. 15 (1), 206-213 (2015). DOI: https://doi.org/10.1016/j.acme.2014.03.003
- [23] C. Qiao, M. Wang, L. Hao, X. Liu, X. Jiang, X. An, D. Li, Temperature and NaCl Deposition Dependent Corrosion of SAC305 Solder Alloy in Simulated Marine Atmosphere. J. Mater. Sci. Technol. 75, 252-264 (2021).
 DOI: https://doi.org/10.1016/j.jmst.2020.11.012
- [24] Y.-F. Gao, C.-Q. Cheng, J. Zhao, L.-H. Wang, X.-G. Li, Electro-chemical Corrosion of Sn–0.75Cu Solder Joints in Nacl Solution. Trans. Nonferrous Met. Soc. China 22 (4), 977-982 (2012). DOI: https://doi.org/10.1016/s1003-6326(11)61273-9